



# Flexible Film-Type Sensor for Electrochemical Measurement of Dopamine Using a Molecular Imprinting Method

Takumi Kishi<sup>1</sup>, Toshinori Fujie<sup>2,3\*</sup>, Hiroyuki Ohta<sup>4</sup> and Shinji Takeoka<sup>1,5\*</sup>

<sup>1</sup>Department of Life Science and Medical Bioscience, School of Advanced Science and Engineering, Waseda University, Shinjuku, Japan, <sup>2</sup>School of Life Science and Technology, Tokyo Institute of Technology, Yokohama, Japan, <sup>3</sup>Research Organization for Nano & Life Innovation, Waseda University, Shinjuku, Japan, <sup>4</sup>Department of Pharmacology, National Defense Medical College, Saitama, Japan, <sup>5</sup>Research Institute for Science and Engineering, Waseda University, Shinjuku, Japan

## OPEN ACCESS

### Edited by:

Bastien Doumeche,  
Université de Lyon, France

### Reviewed by:

Luigi Falcicola,  
University of Milan, Italy  
Gorachand Dutta,  
Indian Institute of Technology  
Kharagpur, India

### \*Correspondence:

Toshinori Fujie  
t\_fujie@bio.titech.ac.jp  
Shinji Takeoka  
takeoka@waseda.jp

### Specialty section:

This article was submitted to  
Electrochemical Sensors,  
a section of the journal  
Frontiers in Sensors

Received: 15 June 2021

Accepted: 07 September 2021

Published: 01 October 2021

### Citation:

Kishi T, Fujie T, Ohta H and Takeoka S  
(2021) Flexible Film-Type Sensor for  
Electrochemical Measurement of  
Dopamine Using a Molecular  
Imprinting Method.  
Front. Sens. 2:725427.  
doi: 10.3389/fsens.2021.725427

Neurotransmitters, which are responsible for the signal transduction of nerve cells in the brain, are linked not only to various emotions and behaviors in our daily life, but also to brain diseases. Measuring neurotransmitters in the brain therefore makes a significant contribution to the progress of brain science. The purpose of this study is to develop a flexible thin film-type sensor that can electrochemically measure dopamine (DA) selectively and with high sensitivity. The thin-film sensor was prepared by printing gold colloidal ink on a polyimide film with a thickness of 25  $\mu\text{m}$ —which the most flexible of the films examined that could maintain the buckling load (1 mN) required for insertion into the brain. The electrode (DA-PPy electrode) was then prepared by electropolymerization of polypyrrole (PPy) using DA as a template. The flexural rigidity of the sensor was  $4.3 \times 10^{-3}$  nNm, which is the lowest of any neurotransmitter sensors reported to date. When a DA solution (0–50 nM) was measured with the DA-PPy electrode using square-wave voltammetry (SWV), the slope of the calibration curve was 3.3 times higher than that of the PPy only negative control electrode, indicating an improvement in sensitivity by molecular imprinting with DA. The sensor was used to measure 0–50 nM norepinephrine (NE) and serotonin (5-HT), and the slope of the DA calibration curve at 0.24 V ( $19 \pm 4.4$  nA/nM) was much greater than those of NE ( $0.99 \pm 3.3$  nA/nM) and 5-HT ( $2.5 \pm 2.4$  nA/nM) because the selectivity for DA was also improved by molecular imprinting.

**Keywords:** molecular imprinting, dopamine, high flexibility, electrochemical sensor, film-type sensor

## INTRODUCTION

Neurotransmitters, which play important roles in the signal transduction of nerve cells in the brain, are linked not only to emotions and behaviors in our daily life, but also to brain diseases such as Parkinson's disease, Huntington's disease, and schizophrenia. Measuring the dynamics of neurotransmitters in the brain therefore makes a significant contribution to the progress of neuroscience (Meder et al., 2019; Niyonambaza et al., 2019). Neurotransmitters include catecholamines such as dopamine, serotonin, epinephrine, and norepinephrine, as well as glutamate and  $\gamma$ -aminobutyric acid (GABA), all of which are small polar molecules. Methods for measuring secreted neurotransmitters include positron emission tomography and optical

detection methods, such as surface-enhanced Raman spectroscopy (SERS), fluorescence, fluorescence resonance energy transfer (FRET), chemiluminescence, column chromatography, and mass spectrometry, used in diagnostic applications; and microdialysis and electrochemical measurement methods, such as cyclic voltammetry and amperometry, used in brain research to quantitatively measure neurotransmitters in the brain (Shariatgorji et al., 2014; Niyonambaza et al., 2019; Patriarchi et al., 2020).

Microdialysis in particular is a widely accepted method for measuring neurotransmitters *in vivo*; however, there are issues associated with collecting excess interstitial fluids, such as limitation of time resolution and destruction of brain homeostasis (Zhang et al., 2013). The electrochemical method, which determines the presence of a target neurotransmitter using a redox reaction of the target molecule with a specific redox potential, is recognized as a method that can overcome these problems (Si and Song, 2018). To measure the electric current derived from the redox reaction of target molecules in brain interstitial fluid, where a large variety of molecules and ions coexist, electrochemical sensors based on enzymes, antibodies, and molecular imprinting polymers that can only bind specific molecules must be developed (Dyke et al., 2017; Crapnell et al., 2019). Sensors that use proteins such as enzymes and antibodies are highly specific but have stability problems.

Molecularly imprinted sensors are sensors in which electrodes are modified with conductive polymers (Gui et al., 2018; Ananthalyengar et al., 2019). Modification with conductive polymers is carried out using a molecular imprinting method in which target molecules are electropolymerized using a mixed solution of monomers and the target molecules, and the target molecules are removed after polymerization to leave templates in the polymer matrix. In contrast to modification with enzymes or antibodies, this approach is resistant to heat, pH changes, and physical shock, and has excellent selectivity as well as being easy to prepare and having a high cost-performance ratio (Crapnell et al., 2019). Various combinations of monomers and target molecules have been reported to date, including dopamine (DA)/polypyrrole (PPy) on a carbon aerogel electrode, norepinephrine/poly-*o*-aminophenol, and epinephrine/poly-2,4,6-triacrylamide-1,3,5-triazine (TAT) (Rosy et al., 2014; Tadi et al., 2015; Yang et al., 2015). There is also a report that a platinum probe modified with dopamine-imprinted polypyrrole was inserted into the striatum of rats and dopamine was successfully measured in the rat brain (Tsai et al., 2012). However, these examples use substrates with high rigidity such as metal probes or silicon wires, and inflammatory reactions accompanying the insertion of the sensor might be a problem for long-term use (Fattahi et al., 2014; Thukral et al., 2018; Hong and Lieber, 2019).

In this study, we develop a flexible thin film-type sensor that can measure dopamine (DA) selectively and with high sensitivity by electrochemical measurement. We focused on a flexible and stable organic material, a polyimide thin film, that has been used in many biomedical devices as a base material of electronic circuits (Takeuchi et al., 2004). PPy was selected as a biocompatible conductive polymer that can be

electropolymerized in an aqueous solvent. The PPy layer was prepared as a molecular imprinted matrix, in which DA was embedded as a template molecule to construct a thin-film electrochemical sensor with high selectivity for DA (Maouche et al., 2012; Yang et al., 2015).

Using inkjet printing, we then made an electrode capable of improving the electrode area by applying gold colloidal aqueous ink (Kokubo et al., 2018). Because aqueous colloidal ink does not adhere to hydrophobic polyimide film following direct application, even after plasma treatment, our strategy was to use an elastomeric thin film consisting of styrene-butadiene-styrene block copolymer (SBS) (Sato et al., 2016) for stable inkjet printing of electrodes and wiring with colloidal ink. Furthermore, the wiring was covered with another SBS nanosheet for insulation. Since the electrode was exposed, a PPy layer was constructed on the electrode by electropolymerization using dopamine as a template. We immersed the obtained electrochemical sensor in a three-electrode electrolytic cell and subjected it to square-wave voltammetry (SWV) to quantify DA in the solution from the change in the measured current and to examine the selectivity of the sensor for DA against norepinephrine (NE) and serotonin (5-hydroxytryptamine; 5-HT).

## MATERIALS AND METHODS

### (1) Printing the gold electrode and wiring on a polyimide/SBS film

Polyimide films (HJA-A4, AS ONE) with thicknesses of 12.5, 25, and 50  $\mu\text{m}$  were purchased, and were cut into rectangles of 1 cm  $\times$  6 cm for use as a base material (**Figure 1A**). The styrene-butadiene-styrene block copolymer (SBS, GF00679361, Sigma-Aldrich) was dissolved in tetrahydrofuran (THF, 20,608,744, Wako Pure Chemical) at a final concentration of 7 wt%, and then an SBS film with a thickness of 5.3  $\mu\text{m}$  was prepared using a benchtop-type bar coater (TC-3, Mitsui Denki Seiki) under 60°C and 2 m/min conditions (**Figure 1B**). SBS was used as primer coating for inkjet printing because gold colloidal ink could not be directly printed on the polyimide film even after plasma treatment. After drying (60°C, 5 min) the bar-coated SBS layer, a plasma treatment (air, 15 W, 3 min) was carried out with a plasma coater (PDC-001, HARRICK PLASMA), and electrodes (0.5 mm<sup>2</sup>) and wiring (200  $\mu\text{m}$   $\times$  4 cm) were printed using an inkjet printer (Dimatix, Fujifilm) with gold colloidal ink (Au-J, C-INK) (**Figure 1C**). Thereafter, a heat treatment (100°C, 1 h) was carried out on a hot plate (HJA-A4, AS ONE) to increase the conductivity. An SBS thin film with thickness of 5.3  $\mu\text{m}$  was formed with the same coater under the same conditions to cover the wiring for insulation (**Figure 1D**) and the electrode was exposed. A razor blade (O39-1CZ, AS ONE) was used to cut the polyimide film into a probe shape with a width of 0.1 mm as shown in **Figure 1E**. Finally, a flexible flat cable (FFC, FFC0508P, Aitendo) was attached to the surface at the end of the wiring using double-sided tape (**Figure 1F**) and connected to the instrument (**Figure 1G**). The cross section of the device is shown in

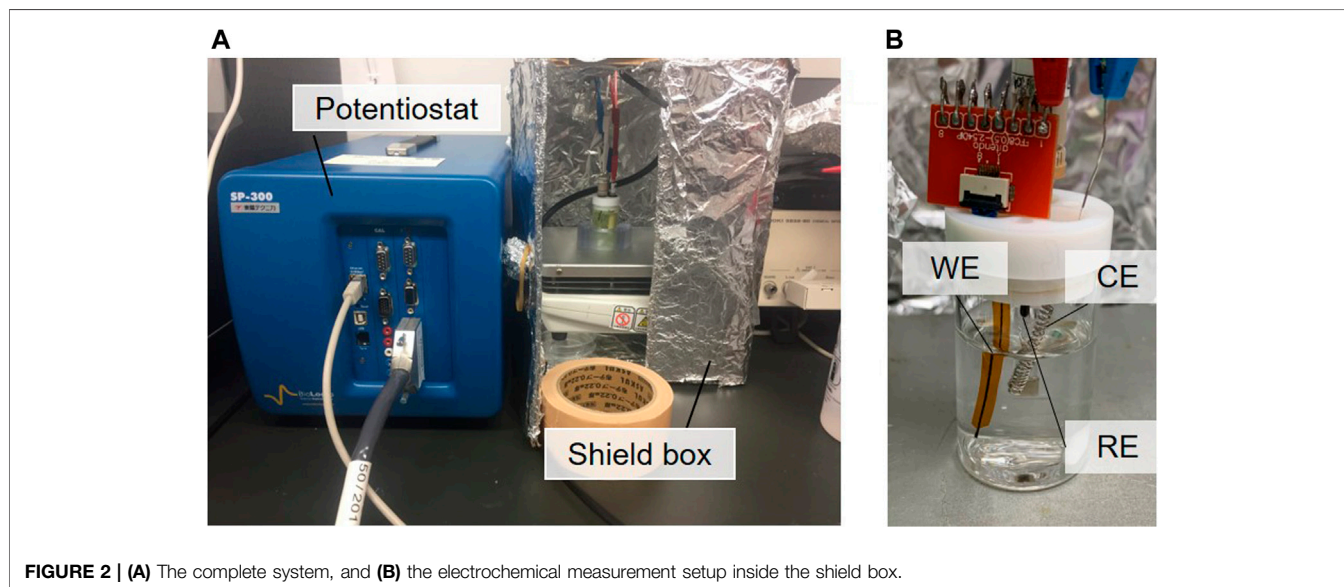
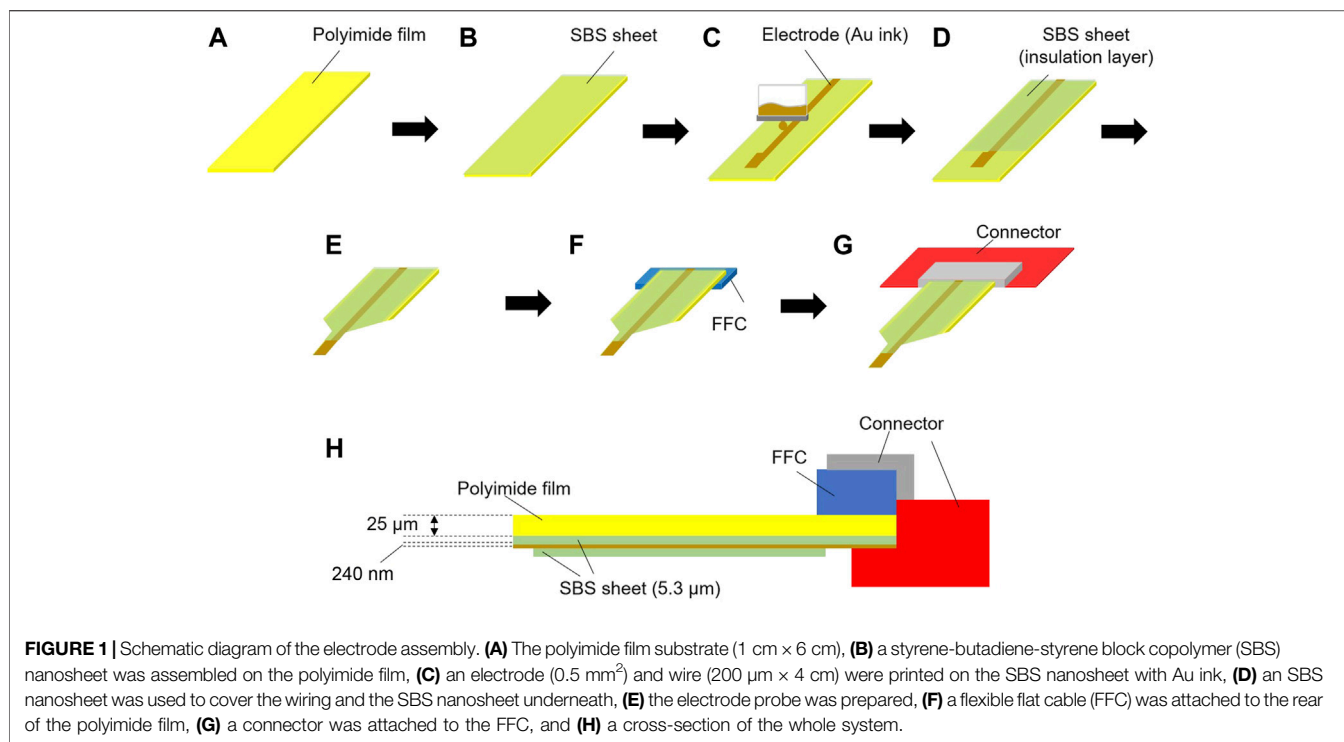


**Figure 1H.** The electrode on the SBS nanosheet was exposed at the tip of the probe and the wiring was sandwiched with another SBS nanosheet for insulation. We used a device that had an impedance at 1 kHz within a 1–5 kΩ range (actual impedance was  $2.59 \pm 1.34$  kΩ) measured using an impedance analyzer (3532–80, HIOKI E.E. Corp.).

(2) Preparation of a molecularly imprinted polypyrrole film on a printed gold electrode

The gold electrode prepared in section *Introduction* was connected to a potentiostat (Toyo Technica, SP-300) as a working electrode, a platinum wire (Nilaco,  $\phi = 0.4$  mm) was used as a counter electrode (CE), and a silver/silver chloride electrode (EC Frontier, RE-2 A) was used as a reference electrode (RE) (**Figure 2A**). All electrodes were immersed in an electropolymerization solution (10 mM pyrrole, 1 mM dopamine hydrochloride, 0.1 M SDS in Milli Q water, N<sub>2</sub> bubbling for 20 min) in an electrochemical cell on a stirrer

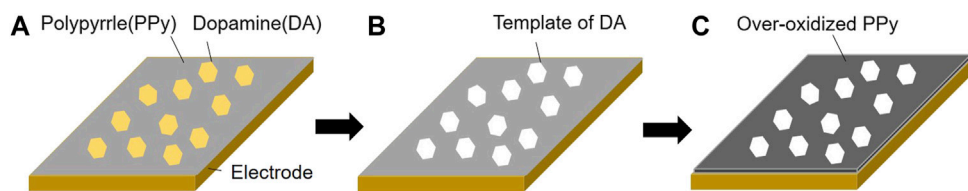


**FIGURE 3** | Schematic diagram of the preparation of the molecularly imprinted polypyrrole (PPy) layer on the gold electrode. **(A)** PPy and dopamine (DA) mixed layer prepared on an electrode by electropolymerization of pyrrole (Py) with DA (scan speed: 10 mV/s, scan range: 0–0.8 V, number of cycles: 3, 100 rpm), **(B)** DA was removed from the mixed layer leaving the DA templates (scan speed: 40 mV/s, scan range: –0.2–0.6 V, number of cycles: 60, 100 rpm), and **(C)** PPy was over-oxidized to improve the conductivity (scan speed: 50 mV/s, scan range: –0.2–1.3 V, number of cycles: 30, 100 rpm).

(**Figure 2B**). The electrochemical cell and stirrer were placed inside a shield box completely covered with aluminum foil to exclude external noise (**Figure 2A**).

Electropolymerization in the solution by cyclic voltammetry (scan speed: 10 mV/s, scan range: 0–0.8 V, number of cycles: 3, 100 rpm) provided a mixed layer of polypyrrole (PPy) and dopamine (DA) on the surface of the gold electrode (**Figure 3A**). The resulting mixed layer was washed with Milli Q, used again as a working electrode, and then a CV sweep (scan speed: 40 mV/s, scan range: –0.2–0.6 V, number of cycles: 60, 100 rpm) was carried out in 0.1 mol/L phosphate buffer, which was thoroughly degassed with nitrogen gas for 20 min, to remove DA from the mixed layer (**Figure 3B**). After the removal of DA, the PPy was washed with Milli Q, and a further CV sweep was carried out over a wider potential range weighted towards oxidation (scan speed: 50 mV/s, scan range: –0.2–1.3 V, number of cycles: 30, 100 rpm), thereby over-oxidizing the PPy layer (**Figure 3C**). Thus, a DA-imprinted and over-oxidized PPy electrode was prepared on the gold electrode (hereafter denoted DA-PPy electrode). In addition, a system in which DA was not added during PPy electropolymerization, processed under the same conditions, was used as a negative control (hereafter denoted PPy electrode).

### (3) Characterization of the DA-imprinted PPy electrode

The electrode before and after electropolymerization was observed using an optical microscope (HOZAN, L-KIT 617). The thickness of the electrode was measured using a stylus-type step gauge (Dektak, Bruker), and the Raman spectrum on the electrode surface was measured with a Raman spectrometer microscope (Japan Spectroscopy, NRS-4100). The tip of the polyimide film (25  $\mu\text{m}$  thickness) bearing a DA-PPy electrode was attached to a substrate and gradually pressurized using a tensile testing machine (EZ-S, Shimadzu Corporation) to bend it. The buckling load was measured when the film buckled.

The quantification of DA in DA solutions was carried out using a three-electrode cell with the DA-PPy electrode as a working electrode. We measured 0–50 nM DA solutions—a range that would not be affected by the Langmuir adsorption isotherm—and the DA concentration and current showed a proportional relationship. Each electrode was immersed in a well-degassed 0.1 mol/L phosphate buffer solution, a 10  $\mu\text{M}$  DA phosphate buffer solution was added to increase the

concentration of DA to 50 nM in 10 nM increments, and a square-wave voltammetry (SWV, scan range: –0.2–0.7 V, pulse height: 25 ms, pulse width: 25 ms, step height: 10 mV) sweep was carried out to measure the change in the oxidation current due to DA in the solution.

To evaluate the selectivity, a DA-PPy electrode was used to measure norepinephrine (NE) or serotonin (5-hydroxytryptamine; 5-HT) in the three-electrode cell. A DA-PPy electrode was used as the working electrode and immersed in a 0.1 mol/L phosphate buffer, and a 10  $\mu\text{M}$  NE or 5-HT phosphate buffer was added to the solution to increase the concentrations of NE or 5-HT to 50 nM in 10 nM steps. The NE or 5-HT oxidation current was measured by carrying out an SWV sweep with each 10 nM increase.

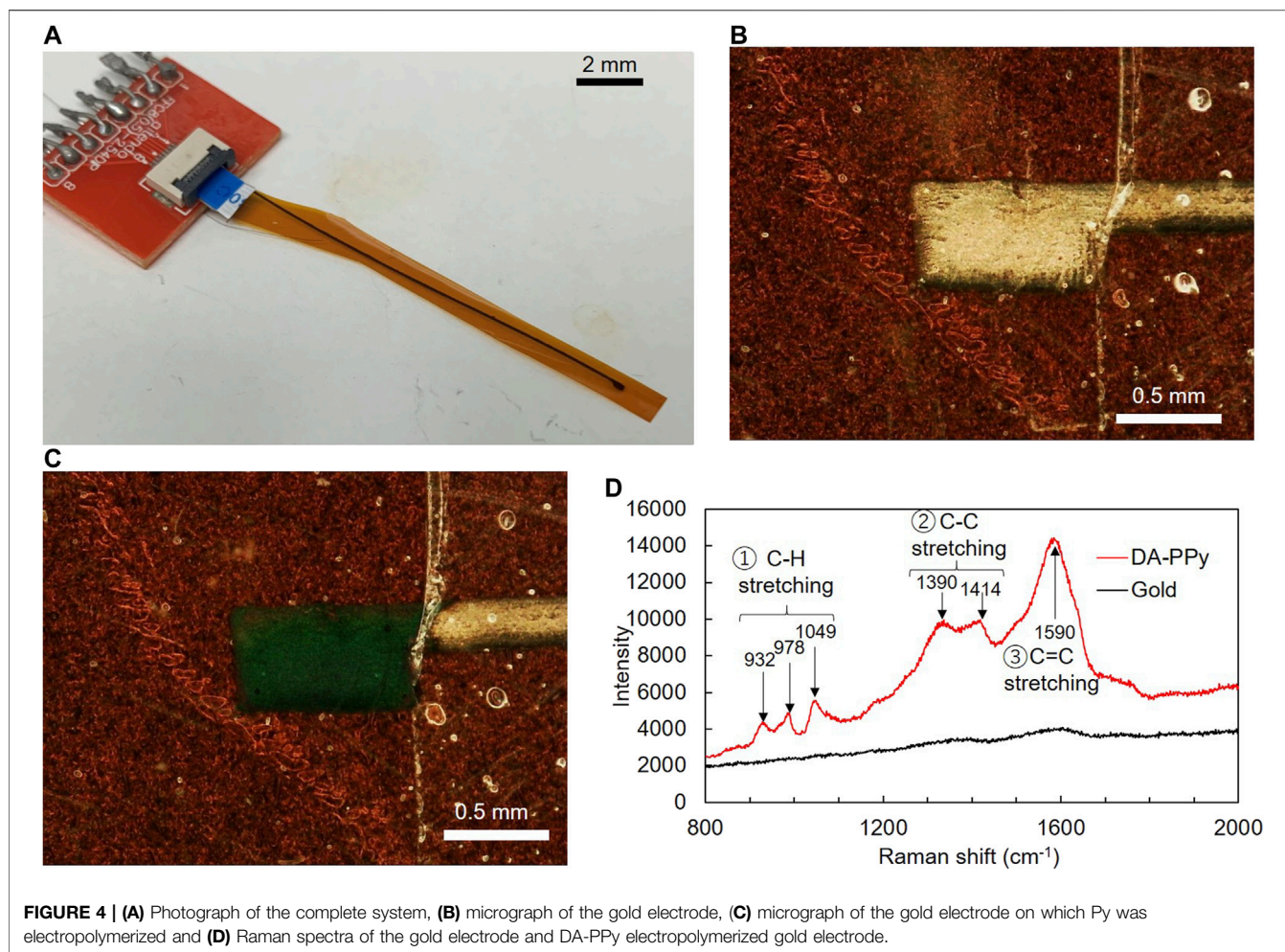
## RESULTS AND DISCUSSION

### Characterization of the Molecularly Imprinted DA-PPy Electrode Appearance

**Figure 4A** shows a photograph of the device. The DA-PPy electrode was electropolymerized on the gold electrode and the wiring was printed on the polyimide thin film. The gold wiring was connected to the connector via the FFC. Magnified images of the printed gold electrode and DA-PPy electrode prepared by electropolymerization are shown in **Figure 4B** and **Figure 4C**, respectively. The wiring was covered with the SBS nanosheet to prevent electropolymerization of PPy, therefore, it appears gold. However, black substances were adsorbed on the exposed gold electrode after electropolymerization.

### Raman Spectrum

**Figure 4D** shows the Raman spectra of the electrode before and after electropolymerization. No major peaks were observed in the Raman spectrum of the bare surface of the gold electrode before the electropolymerization; however, after the electropolymerization, numerous peaks appeared in the spectrum, including peaks at 932, 978, and 1,049  $\text{cm}^{-1}$  assigned to C-H stretching and 1,390 and 1,414  $\text{cm}^{-1}$  assigned to C-C stretching and 1,590  $\text{cm}^{-1}$  assigned to C=C stretching. A typical Raman spectrum of PPy from the literature confirmed that the black substance formed on the surface of the gold electrode after the electropolymerization was polypyrrole (Tsai et al., 2012).

**TABLE 1 |** Configuration of the PA-PPy electrode system.

Layers	$h$ ( $\mu\text{m}$ )	$E$ (GPa)	$D$ ( $\text{nN} \cdot \text{m}$ )
Polyimide Film	25	3.3	$4.30 \times 10^3$
Bar-coated SBS Layer	5.3	$5.7 \times 10^{-3}$	0.566
Printed Gold Layer	$2.4 \times 10^{-3}$	78	$8.99 \times 10^{-2}$
Electropolymerized PPy Layer	0.135	1.2	$2.46 \times 10^{-4}$

### Film Thickness and Flexural Rigidity

Measurement using Dektak showed a printed gold electrode thickness of  $236 \pm 40$  nm, which increased to  $371 \pm 44$  nm after electropolymerization. Therefore, the thickness of the DA-PPy electrode was calculated to be  $135 \pm 43$  nm. For inkjet-printed electrodes it is difficult to control the consistency of the surface roughness and impedance for each fabrication. This may affect the molecular imprinting of DA on PPy even under the same fabrication conditions, which include the concentration of monomer (Py), DA, and supporting electrolyte (SDS); scan speed, scan range, and cycle number for the cyclic voltammetry; temperature; and stirring speed. The SBS layer formed by the bar coater had a thickness of

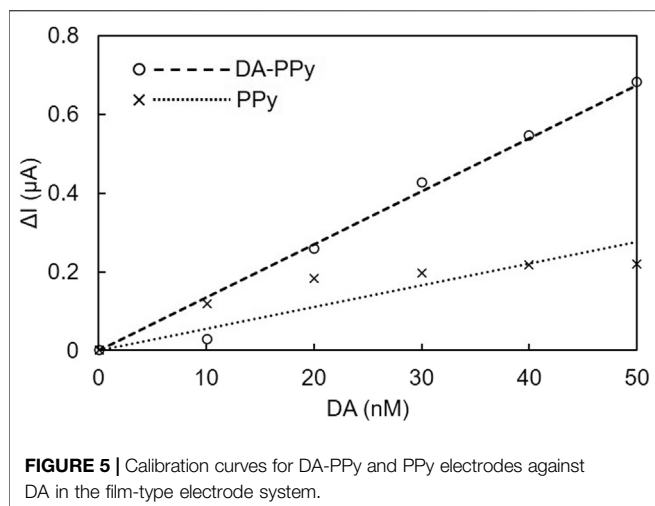
**TABLE 2 |** Comparison of the flexural rigidity of the substrate of brain insertion-type electrodes in this study and previous studies.

Studies	Materials	Size ( $\mu\text{m}$ )	$D$ ( $\text{nN} \cdot \text{m}$ )
Robinson <i>et al.</i> (2003)	Carbon	$\Phi = 30$	$2.2 \times 10^5$
Suzuki <i>et al.</i> (2007)	Diamond	$\Phi = 5$	$1.0 \times 10^5$
Tsai <i>et al.</i> (2012)	Platinum	$\Phi = 25$	$7.9 \times 10^5$
This work	PI films	$100 \times 30.8$	$0.043 \times 10^5$
Brain tissue [Yamagishi <i>et al.</i> , (2019)]	—	—	1.0

5.3  $\mu\text{m}$ . The configuration of the PA-PPy electrode constructed on the polyimide thin film is shown in **Table 1**, and the value of flexural rigidity,  $D$ , calculated from the thickness,  $h$ , and Young's modulus,  $E$ , of each constituent layer was calculated using **Eq. 1** (Yamagishi *et al.*, 2019).

$$D = \frac{Eh^3}{12(1-\nu^2)} \quad (1)$$

$D$ : Flexural rigidity (N m),  $E$ : Young's modulus ( $\text{N}/\text{m}^2$ ),  $h$ : Thickness (m),  $\nu$ : Poisson's ratio.



Comparison of the  $D$  value of each layer suggested that the flexural rigidity of the complete DA-PPy electrode system constructed on the 25  $\mu\text{m}$  thick polyimide thin film could be given by the  $D$  value of the polyimide film, and was estimated to be  $4.30 \times 10^3 \text{ nNm}$ .

**Table 2** shows a comparison of the substrate, electrode size, and flexural rigidity,  $D$ , of brain insertion-type electrodes. The  $D$  values in this study, which were determined based on a polyimide film substrate with a thickness of 25  $\mu\text{m}$ , are two orders of magnitude lower than those of previously reported substrates. However, it is still three orders of magnitude more rigid than brain tissue. It is not yet clear what difference in stiffness between the substrate and brain tissue will be appropriate for application of the electrode in the brain. This will be investigated by changing the thickness of the polyimide film substrate.

### Buckling Load

The polyimide film with a thickness of 25  $\mu\text{m}$  had a buckling load of 3.65 mN. The buckling loads for film with thicknesses of 50  $\mu\text{m}$  and 12.5  $\mu\text{m}$ , were 12.3 mN and less than 1 mN, respectively. Assuming that the electrodes will be used by inserting them into the brain, buckling loads of 1 mN or more are required (Jensen and Yoshida, 2003). Therefore, the polyimide film with 25  $\mu\text{m}$  thickness was considered a suitable substrate.

### Selective DA Measurements Using DA-PPy Electrodes

We first evaluated the surface area of the electrode, and as a result decided to use a 0.5  $\text{mm}^2$  electrode because it was the smallest size capable of measuring DA with high reproducibility (see **Supplementary Material**). In addition, we used  $\Delta I$  (calculated by  $I - I_0$ ,  $I$ : measured current of each DA concentration (10–50 nM),  $I_0$ : current of DA at 0 nM) and evaluated the sensitivity as  $\Delta I/\Delta C$  (concentration increase) from the slope of the relationship between  $\Delta I$  and DA concentration. Calibration curves of the DA-PPy electrode and PPy electrode from the current values at 0.24 V are shown in **Figure 5**. The average slopes based on three measurements were  $19 \pm 4.4 \text{ nM}$  (DA-PPy) and

$6.0 \pm 5.7 \text{ nA/nM}$  (PPy). The sensitivity of the DA-PPy electrode was 3.3 times higher than that of the control, which is attributed to the increase in the amount of DA adsorbed on the electrode surface as a result of the DA molecular imprinting. For reference, we preliminarily used bar-type glassy carbon electrodes instead of film-type electrodes. The slopes of the DA-PPy-modified glassy carbon electrodes were approximately 3 times greater than those of the PPy-modified glassy carbon electrode, which indicates a similar DA templating effect to that observed for the film-type electrodes (See **Supplementary Material**).

High concentrations of neurotransmitters (DA, NE, and 5-HT) were measured using SWV to determine the oxidation potential of each transmitter. A voltammogram of 5,000 nM DA, NE, and 5-HT using a DA-PPy electrode is shown in **Figure 6**. Oxidation potentials were observed at 0.24 V for DA and NE and at  $-0.09 \text{ V}$  for 5-HT. The same oxidation potential was also observed for each neurotransmitter in the case of glassy carbon electrodes (see **Supplementary Material**). These results suggest that it is difficult to detect DA in a mixture of DA and NE by changing the oxidation potential for observation because the oxidation potential of NE is almost the same as that of DA.

The SWV voltammograms of DA, NE, and 5-HT in the low concentration range are shown in **Figure 7A**, **Figure 7B**, and **Figure 7C**, respectively. No oxidation peak was confirmed for NE and 5-HT in this concentration range (0–50 nM). For DA, the  $I$  values of the whole curve (approximately 0.1–0.3 V) increased as the DA concentration increased. As this was in the same range as the oxidation peak shown in **Figure 6**, the oxidation peak appeared. The calibration curves shown in **Figure 7D** were prepared based on the oxidation potential of DA (0.24 V). Only the calibration curve of DA at 0.24 V had a significant slope. No distinct slopes were observed for NE or 5-HT at 0.24 V, or for 5-HT at  $-0.09 \text{ V}$ .

From the slopes of the calibration curves of **Figure 7D** it can be seen that the slope for DA ( $19 \pm 4.4 \text{ nA/nM}$ ) was greater than those for NE ( $0.93 \pm 3.3 \text{ nA/nM}$ ) and 5-HT ( $2.5 \pm 2.4 \text{ nA/nM}$ ), despite each organic thin-film sensor being fabricated under the same conditions. A similar trend for selectivity was also found in the case

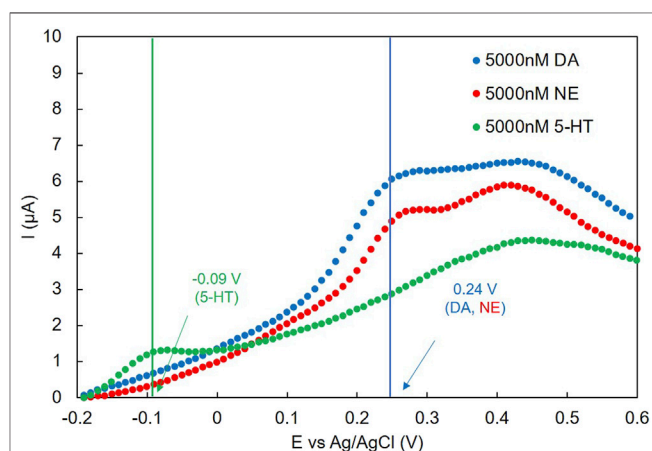


**FIGURE 6** | SWV voltammogram of concentrated DA, NE, and 5-HT with DA-PPy electrodes.

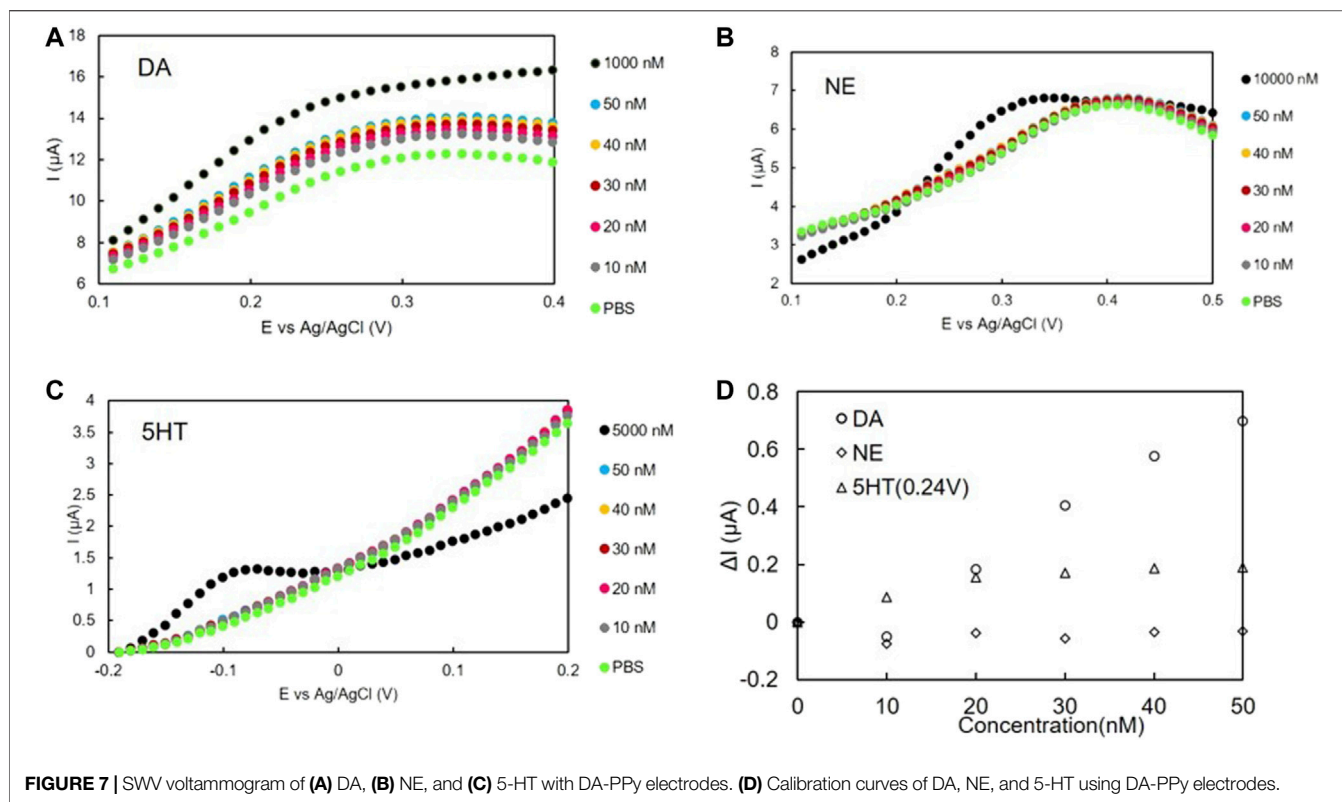


**TABLE 3 |** Comparison with previous studies.

Studies	Material	S (mm <sup>2</sup> )	L (nA/nM)	L/S (nA/(nM · mm <sup>2</sup> ))	Selectivity
This work	PPy/Au	0.5	19	38	AA, UA, NE, 5-HT
Tsai et al. (2012)	PPy/Pt	1.2	17	14	AA, DOPAC, 5-HT
Yang et al. (2015)	PPy/carbon aerogel	3.0 × 10 <sup>3</sup>	4.0	1.3 × 10 <sup>-3</sup>	AA, UA, NE, EP
Si et al. (2011)	PPy/eRGO	7.1	4.0 × 10 <sup>-2</sup>	5.6 × 10 <sup>-3</sup>	AA, UA
Zhang et al. (2013)	Nafion/PtNPs/Pt	0.126	1.3 × 10 <sup>-4</sup>	1.0 × 10 <sup>-4</sup>	AA, UA, DOPAC
Chen et al. (2019)	Au nanoparticle/rGO/Pt	3.1	0.261	8.4 × 10 <sup>-2</sup>	AA, UA, Glucose, Glutamate

of the glassy carbon electrode, namely, the slope of the calibration curve of DA was 6 times greater than those of NE and 5-HT (see **Supplementary Material**). We also confirmed that ascorbic acid (AA) and uric acid (UA) did not interfere with the measurement (see **Supplementary Material**). It is therefore thought that imprinting with DA improves the detection sensitivity of DA over NE at the same oxidation potential. These results indicate that the sensitivity of DA at 0.24 V using the DA-PPy electrode is sufficiently higher than those of NE and 5-HT; therefore, the DA concentration change can be selectively measured even in the presence of NE or 5-HT. In addition, the surface area (S), the slope of the calibration curve for DA measurement (L), and the L/S value were compared with previous research as summarized in **Table 3**.

**Table 3** shows that the organic thin-film sensor has a higher L/S value those reported for other systems. This means that the sensitivity of the organic-thin film is higher than those of other studies in terms of unit area. This increase in sensitivity is attributed to the high surface area of the electrode due to the

Au nanoparticles of the Au colloidal ink. These results indicate that the organic thin-film sensor can detect DA with high sensitivity. The DA concentration of brain interstitial fluid is reported to be 2–4 nM (Chatard et al., 2018). The organic thin-film sensor was able to measure 10 nM DA. Optimization of the electropolymerization conditions is therefore necessary to increase the sensitivity for measuring DA *in vivo*.

## CONCLUSION

An organic thin-film sensor based on a 25 μm-thick polyimide film was prepared, which is flexible and can be inserted into the mouse brain. The sensor was found to be more flexible than all neurotransmitter sensors reported to date. The molecularly imprinted polymer sensor showed improved DA detection sensitivity both as an organic thin film and as a glassy carbon electrode. DA could be measured with high sensitivity and

selectivity even in the presence of NE and 5-HT. In future, inkjet-printed channels for the CE and RE will be loaded onto the organic thin-film sensor to develop 3-channel sensors for DA measurement in the brain without inserting a separate CE and RE (Chatard et al., 2018). In addition, we plan to evaluate the toxicity of the organic thin-film sensor materials. And we intend to carry out *in vivo* experiments to measure the DA secreted by operant behavior by inserting the sensor into the striatum of mice or rats under acute conditions (in 1 h).

## DATA AVAILABILITY STATEMENT

The raw data supporting the conclusions of this article will be made available by the authors, without undue reservation.

## AUTHOR CONTRIBUTIONS

TF designed the experiments with HO, TK conducted the experiments and TF and HO directed the experiments. ST described the manuscript with TK.

## REFERENCES

- Anantha-Iyengar, G., Shanmugasundaram, K., Nallal, M., Lee, K.-P., Whitcombe, M. J., Lakshmi, D., et al. (2019). Functionalized conjugated polymers for sensing and molecular imprinting applications. *Prog. Polym. Sci.* 88, 1–129. doi:10.1016/j.progpolymsci.2018.08.001
- Chatard, C., Meiller, A., and Marinesco, S. (2018). Microelectrode Biosensors for *in vivo* Analysis of Brain Interstitial Fluid. *Electroanalysis* 30, 977–998. doi:10.1002/elan.201700836
- Chen, X., Chen, J., Dong, H., Yu, Q., Zhang, S., and Chen, H. (2019). Sensitive detection of dopamine using a platinum microelectrode modified by reduced graphene oxide and gold nanoparticles. *J. Electroanalytical Chem.* 848, 113244. doi:10.1016/j.jelechem.2019.113244
- Crapnell, R., Hudson, A., Foster, C., Eersels, K., Grinsven, B., Cleij, T., et al. (2019). Recent advances in electrosynthesized molecularly imprinted polymer sensing platforms for bioanalyte detection. *Sensors* 19, 1204. doi:10.3390/s19051204
- Dyke, K., Pépés, S. E., Chen, C., Kim, S., Sigurdsson, H. P., Draper, A., et al. (2017). Comparing GABA-dependent physiological measures of inhibition with proton magnetic resonance spectroscopy measurement of GABA using ultra-high-field MRI. *Neuroimage* 152, 360–370. doi:10.1016/j.neuroimage.2017.03.011
- Fattahi, P., Yang, G., Kim, G., and Abidian, M. R. (2014). A review of organic and inorganic biomaterials for neural interfaces. *Adv. Mater.* 26, 1846–1885. doi:10.1002/adma.201304496
- Gui, R., Jin, H., Guo, H., and Wang, Z. (2018). Recent advances and future prospects in molecularly imprinted polymers-based electrochemical biosensors. *Biosens. Bioelectron.* 100, 56–70. doi:10.1016/j.bios.2017.08.058
- Hong, G., and Lieber, C. M. (2019). Novel electrode technologies for neural recordings. *Nat. Rev. Neurosci.* 20, 330–345. doi:10.1038/s41583-019-0140-6
- Jensen, W., and Yoshida, K. (2003). Subdural Insertion Force. *Area*, 2168–2171.
- Kokubo, N., Arake, M., Yamagishi, K., Morimoto, Y., Takeoka, S., Ohta, H., et al. (2018). Inkjet-Printed Neural Electrodes with Mechanically Gradient Structure. *ACS Appl. Bio Mater.* 2, 20–26. doi:10.1021/acsabm.8b00574
- Maouche, N., Guergouri, M., Gam-Derouich, S., Jouini, M., Nessark, B., and Chehimi, M. M. (2012). Molecularly imprinted polypyrrole films: Some key parameters for electrochemical picomolar detection of dopamine. *J. Electroanalytical Chem.* 685, 21–27. doi:10.1016/j.jelechem.2012.08.020
- Meder, D., Herz, D. M., Rowe, J. B., Lehericy, S., and Siebner, H. R. (2019). The role of dopamine in the brain - lessons learned from Parkinson's disease. *Neuroimage* 190, 79–93. doi:10.1016/j.neuroimage.2018.11.021

## FUNDING

This work was supported by JSPS KAKENHI (grant number 18H03539, 18H05469, 21H03815) from MEXT, Japan, the Tanaka Memorial Foundation, and Fusion Oriented REsearch for disruptive Science and Technology (FOREST) (grant number JPMJFR203Q); Japan Science and Technology Agency. TF is supported by the Leading Initiative for Excellent Young Researchers (LEADER) from MEXT, Japan.

## ACKNOWLEDGMENTS

We thank Sarah Dodds, PhD, from Edanz (<https://jp.edanz.com/ac>) for editing a draft of this manuscript.

## SUPPLEMENTARY MATERIAL

The Supplementary Material for this article can be found online at: <https://www.frontiersin.org/articles/10.3389/fsens.2021.725427/full#supplementary-material>

- Niyonambaza, S. D., Kumar, P., Xing, P., Mathault, J., De Koninck, P., Boisselier, E., et al. (2019). A Review of neurotransmitters sensing methods for neuro-engineering research. *Appl. Sci.* 9, 4719–4731. doi:10.3390/app9214719
- Patriarchi, T., Mohebi, A., Sun, J., Marley, A., Liang, R., Dong, C., et al. (2020). An expanded palette of dopamine sensors for multiplex imaging *in vivo*. *Nat. Methods* 17, 1147–1155. doi:10.1038/s41592-020-0936-3
- Robinson, D. L., Venton, B. J., Heien, M. L. A. V., and Wightman, R. M. (2003). Detecting subsecond dopamine release with fast-scan cyclic voltammetry *in vivo*. *Clin. Chem.* 49, 1763–1773. doi:10.1373/49.10.1763
- Rosy, Chasta, H., and Goyal, R. N. (2014). Molecularly imprinted sensor based on o-aminophenol for the selective determination of norepinephrine in pharmaceutical and biological samples. *Talanta* 125, 167–173. doi:10.1016/j.talanta.2014.02.038
- Sato, N., Murata, A., Fujie, T., and Takeoka, S. (2016). Stretchable, adhesive and ultra-conformable elastomer thin films. *Soft Matter* 12, 9202–9209. doi:10.1039/C6SM01242F
- Shariatgorji, M., Nilsson, A., Goodwin, R. J. A., Källback, P., Schintu, N., Zhang, X., et al. (2014). Direct targeted quantitative molecular imaging of neurotransmitters in brain tissue sections. *Neuron* 84, 697–707. doi:10.1016/j.neuron.2014.10.011
- Si, B., and Song, E. (2018). Recent advances in the detection of neurotransmitters. *Chemosensors* 6, 1–24. doi:10.3390/chemosensors6010001
- Si, P., Chen, H., Kannan, P., and Kim, D.-H. (2011). Selective and sensitive determination of dopamine by composites of polypyrrole and graphene modified electrodes. *Analyst* 136, 5134–5138. doi:10.1039/c1an15772h
- Suzuki, A., Ivandini, T. A., Yoshimi, K., Fujishima, A., Oyama, G., Nakazato, T., et al. (2007). Fabrication, characterization, and application of boron-doped diamond microelectrodes for *in vivo* dopamine detection. *Anal. Chem.* 79, 8608–8615. doi:10.1021/ac071519h
- Tadi, K. K., Motghare, R. V., and Ganesh, V. (2015). Electrochemical detection of epinephrine using a biomimic made up of hemin modified molecularly imprinted microspheres. *RSC Adv.* 5, 99115–99124. doi:10.1039/c5ra16636e
- Takeuchi, S., Suzuki, T., Mabuchi, K., and Fujita, H. (2004). 3D flexible multichannel neural probe array. *J. Micromech. Microeng.* 14, 104–107. doi:10.1088/0960-1317/14/1/014
- Thukral, A., Ershad, F., Enan, N., Rao, Z., and Yu, C. (2018). Soft Ultrathin Silicon Electronics for Soft Neural Interfaces: A Review of Recent Advances of Soft Neural Interfaces Based on Ultrathin Silicon. *IEEE Nanotechnology Mag.* 12, 21–34. doi:10.1109/MNANO.2017.2781290

- Tsai, T.-C., Han, H.-Z., Cheng, C.-C., Chen, L.-C., Chang, H.-C., and Chen, J.-J. J. (2012). Modification of platinum microelectrode with molecularly imprinted over-oxidized polypyrrole for dopamine measurement in rat striatum. *Sensors Actuators B: Chem.* 171-172, 93–101. doi:10.1016/j.snb.2011.07.052
- Yamagishi, K., Takeoka, S., and Fujie, T. (2019). Printed Nanofilms Mechanically Conforming to Living Bodies. *Biomater. Sci.* 7, 520–531. doi:10.1039/C8BM01290C
- Yang, Z., Liu, X., Wu, Y., and Zhang, C. (2015). Modification of carbon aerogel electrode with molecularly imprinted polypyrrole for electrochemical determination of dopamine. *Sensors Actuators B: Chem.* 212, 457–463. doi:10.1016/j.snb.2015.02.057
- Zhang, J., Jaquins-Gerstl, A., Nesbitt, K. M., Rutan, S. C., Michael, A. C., and Weber, S. G. (2013). *In Vivo* monitoring of serotonin in the striatum of freely moving rats with one minute temporal resolution by online microdialysis-capillary high-performance liquid chromatography at elevated temperature and pressure. *Anal. Chem.* 85, 9889–9897. doi:10.1021/ac4023605

**Conflict of Interest:** The authors declare that the research was conducted in the absence of any commercial or financial relationships that could be construed as a potential conflict of interest.

**Publisher's Note:** All claims expressed in this article are solely those of the authors and do not necessarily represent those of their affiliated organizations, or those of the publisher, the editors and the reviewers. Any product that may be evaluated in this article, or claim that may be made by its manufacturer, is not guaranteed or endorsed by the publisher.

Copyright © 2021 Kishi, Fujie, Ohta and Takeoka. This is an open-access article distributed under the terms of the Creative Commons Attribution License (CC BY). The use, distribution or reproduction in other forums is permitted, provided the original author(s) and the copyright owner(s) are credited and that the original publication in this journal is cited, in accordance with accepted academic practice. No use, distribution or reproduction is permitted which does not comply with these terms.